Development and Validation of Scaled Electric Combat Vehicle Virtual Model

by

Glenn Xavier Vaz

A Major Project submitted to the
School of Graduate and Postdoctoral Studies in partial
fulfillment of the requirements for the degree of

Masters of Engineering in Automotive Engineering

Faculty of Engineering and Applied Sciences

University of Ontario Institute of Technology (Ontario Tech University)

Oshawa, Ontario, Canada

November, 2023

© Glenn Xavier Vaz, 2023

MAJOR PAPER REVIEW INFORMATION

Submitted by: **Glenn Xavier Vaz**

Masters of Engineering in **Automotive Engineering**

Project/Major Paper title: Development and Validation of Scaled Electric Combat Vehicle Virtual Model

The Major Project was approved on November 3, 2023 by the following review committee:

Review Committee:

Research Supervisor	DR. ZEINAB EL-SAYEGH
Second Reader	DR. MOUSTAFA EL-GUINDY

The above review committee determined that the Major Project is acceptable in form and content and that a satisfactory knowledge of the field was covered by the work submitted. A copy of the Certificate of Approval is available from the School of Graduate and Postdoctoral Studies.

ABSTRACT

This research focuses on an 8x8 scaled electric combat vehicle (SECV) and aims to create a virtual model made of the same vehicle on a vehicle dynamics simulation software using parameters from the actual vehicle. In the proposed vehicle, each wheel is independently driven and steered. MATLAB and Simulink software were used to design and implement the electric powertrain while TruckSim Modelling and Simulation software was used to simulate the on-road conditions tests. The simulation data was then compared with the experimental data obtained from the physical test scenarios.

Keywords: TruckSim; MATLAB; Wheel angle; Yaw Rate; Longitudinal Velocity

ACKNOWLEDGEMENTS

My project supervisor, Dr. Zeinab El-Sayegh, has provided me with tremendous direction, constant support, and wide experience throughout this project, for which I am really grateful. Her extensive expertise in vehicle dynamics and her unwavering drive have been important in determining the project's course.

Dr. El-Sayegh's insightful comments, helpful criticism, and painstaking attention to particulars have greatly enhanced the element analysis, experimental design, and result interpretation. Her support and guidance have been crucial in improving the caliber of this scientific work.

Additionally, I want to thank my research partner, Junwoo Kim, for his cooperation, help, and informative discussions. His ideas and efforts have improved the project as a whole and made it easier to comprehend the subject matter thoroughly.

In addition, I would like to thank Dr. Moustafa El-Guindy, the department and the university for providing the facilities and necessary resources that made this research possible to be completed successfully.

Lastly, I want to express my gratitude to friends and family for their unwavering understanding, encouragement, and support during this project. Their confidence in my skills and constant drive have been a major source of inspiration for me while I've conducted my studies.

Without the joint efforts, direction, and assistance of all the aforementioned people, this task wouldn't have been feasible. Their invaluable contributions have been vital in the effective production of this major project.

STATEMENT OF CONTRIBUTIONS

I hereby certify that I am the sole author of this work and that no part of this work has been published or submitted for publication. I have used standard referencing practices to acknowledge ideas, research techniques, or other materials that belong to others. Furthermore, I hereby certify that I am the sole source of the creative works and/or inventive knowledge described in this document.

TABLE OF CONTENTS

MAJOR PAPER REVIEW INFORMATION ..... **ii**
ABSTRACT ..... **iii**
ACKNOWLEDGEMENTS ..... **iv**
STATEMENT OF CONTRIBUTIONS ..... **v**
TABLE OF CONTENTS ..... **vi**
LIST OF TABLES ..... **vii**
LIST OF FIGURES ..... **viii**
LIST OF ABBREVIATIONS ..... **ix**
Chapter 1. Introduction **1**
Chapter 2. Modelling of the Scaled Electric Combat Vehicle **5**
2.1 Physical Parameters of Scaled Electric Combat Vehicle (SECV) 5
2.2 Motor Specifications inputted into MATLAB. 9
2.2.1 MATLAB inputs. 10
2.3 *Powertrain Design Implemented in Simulink* 10
2.3.1 General Architecture 11
2.3.2 Vehicle Velocity Controller Block Design 11
2.3.3 Motor Block Design 12
Chapter 3. Validation of the Scaled Electric Combat Vehicle **15**
3.1 Vehicle Model and Test Apparatus Specifications 15
3.2 Test Setup Specifications 16
Chapter 4. Results and Discussions **18**
4.1 Double Lane Change Test at 1km/h. 18
4.2 Double Lane Change Test at 2km/h 23
Chapter 5. Conclusions and Future Work **27**
REFERENCES **28**

LIST OF TABLES

Table 1. Measured Parameters of SECV 7
Table 2. Specifications of each motor used. 9

LIST OF FIGURES

Figure 1-1. Prototype model of the Scaled Electric Combat Vehicle [6] 2
Figure 1-2. Electric powertrain implemented in the Scaled Electric Combat Vehicle [6] . 3
Figure 1-3. Block diagram of PID controller [11] 4
Figure 2-1. Ackermann Steering for 1st and 2nd axle steering 8
Figure 2-2. Absolute longitudinal tire force of each tire..... 8
Figure 2-3. Absolute Lateral Force for each tire..... 9
Figure 2-4. Aligning Moment induced in each tire..... 9
Figure 2-5. Output Torque vs Current vs RPM of each motor. 10
Figure 2-6. General Architecture of Simulink file developed. 11
Figure 2-7. Simulink Architecture for motor current derivation 11
Figure 2-8. Simulink Architecture for individual motor..... 13
Figure 2-9. Simulink Architecture for electric powertrain 14
Figure 3-1. Schematic of path setup for the Double Lane Change (DLC) test..... 16
Figure 3-2. (a) Simulation and (b) Experimental path followed by the SECV..... 17
Figure 4-1. Rate of experimental velocity and simulation velocity at 1km/h..... 19
Figure 4-2. Angles induced in each wheel during experiment at 1km/h. 20
Figure 4-3. Angles induced in each wheel during simulation at 1km/h. 20
Figure 4-4. Yaw rate experienced in the vehicle during experiment at 1km/h..... 21
Figure 4-5. Yaw rate experienced in the vehicle during simulation at 1km/h..... 22
Figure 4-6. Comparison of yaw rates during Experiment vs Simulation at 1km/h 22
Figure 4-7. Rate of experimental velocity and simulation velocity at 2km/h..... 23
Figure 4-8. Angles induced in each wheel during experiment at 2km/h. 24
Figure 4-9. Angles induced in each wheel during simulation at 2km/h. 24
Figure 4-10. Yaw rate experienced in the vehicle during experiment at 2km/h..... 25
Figure 4-11. Yaw rate experienced in the vehicle during simulation at 2km/h..... 26
Figure 4-12. Comparison of yaw rates during Experiment vs Simulation at 2km/h 26

LIST OF ABBREVIATIONS

ABS	Absolute Braking System
ARS	Active Rear-axle Steering
CG	Center of Gravity
DLC	Double Lane Change
DoF	Degree of Freedom
LQG	Linear Quadratic Gauss
LQR	Linear Quadratic Regulator
PD	Degree of Freedom
PID	Proportional–Integral–Derivative
SECV	Scaled Electric Combat Vehicle
SIL	Software-In-the-Loop
SISO	Single-Input-Single-Output
TCS	Traction Control System
TVC	Torque Vectoring Controller
ZSS	Zero Side Slip

Chapter 1. Introduction

The field of software testing continues to evolve, and model-based virtual testing has become one of the most important parts of modern test automation. With virtual testing, the parameters and constraints of a test can be easily varied with minimum adjustments without the use of a real-life model. This contributes to lower costs and time savings, which makes virtual testing one of the most sought-after methods in the automotive industry. The vehicle studied in this research is an 8x8 combat vehicle powered by a diesel engine with steering induced in the first two axles of the vehicle. In 2014, Hossam [1]. developed and validated a full-scale model for the 22 Degree of Freedom (DoF) 8x8 combat vehicle in TruckSim using the data provided by General Dynamics Land Systems – Canada. The vehicle was developed in MATLAB/Simulink and was validated using four different test courses including Double Lane Change; Constant Step Slalom; J-Turn with the 8x4 powertrain drive; and the Turning circle test with the 8x8 and 8x4 configuration powertrain. Hossam improved the vehicle's directional stability and maximum traction available while reducing the possibility of a rollover using a developed yaw rate controller, fuzzy slip controller, and an integrated (yaw- fuzzy slip) controller. Corrective torques were introduced in individual tires to improve the turning characteristics of the vehicle. This successful torque control strategy carried out in the study can be implemented in a multi-axle vehicle. It was suggested that more research was needed to implement an electric powertrain to improve the use of the torque vectoring control strategy.

In 2016, D'Usro et al.[2] developed a torque vectoring method for the full scale vehicle along with multiple steering techniques. The proposed technique was a H∞ linear control technique for MIMO systems. With this technique, an Active steering strategy, the torque vectoring method and an integrated controller were developed. The proposed technique proved to be better than the LQG (Linear Quadratic Gauss) controller due to its robustness and disturbance rejection, both of which are essential at high speed controls of the vehicle. During the same year, a scaled down physical prototype model was being developed to allow for further testing of the vehicle. This prototype consisted of the powertrain model highlighted in the research.

In 2017, Arnold et al.[3] converted the pre-mentioned diesel-powered vehicle to an electric vehicle. With the previous additions, this model consisted of an electric powertrain. Similar to Omar's proposed full-scale combat vehicle [4], this model has eight separate actuators controlling each wheel, as well as independent motors for each wheel. The vehicle uses multiple controllers (all developed in MATLAB/ Simulink) to achieve forward thrust, vehicle stability, and steering mechanisms. It also contains an autonomous control unit for lower speeds. It uses a torque distribution controller for its electric powertrain to distribute power to each wheel motor. Multiple tests (Double Lane Change, Fishhook, Off Off-road, etc.) were conducted for low and high speeds on different road conditions. An LQR Active Yaw controller was developed and compared to a Feed-forward controller for the low-speed tests. An LQR torque vectoring controller with various steering mechanisms was

tested for higher speeds. The final result was an all-electric virtual full scale model of the actual 8x8 diesel power model developed by previous literature [1].

In 2018, Russell [5] used the above-validated virtual model to develop a rear axle steering controller for the full scaled vehicle. Brett discussed two main control methods including the Zero Side Slip (ZSS) feed-forward controller and the Linear Quadratic Regulator (LQR) optimal controller. The controllers were developed using MATLAB/ Simulink and were tested under five different tests including the 15m slalom, 100 feet radius circle w/constant acceleration, modified J-turn, FMVSS 126 ESC, and the NATO double lane change. The ZSS controller was successful for lower speeds while the LQR controller excelled at higher speeds.

Figure 1-1. Prototype model of the Scaled Electric Combat Vehicle [6]

In 2019, Tan [6] completed the aforementioned prototype scaled electric combat vehicle of the pre-mentioned vehicle. The main aim of the research was to design and develop an autonomous scaled electric combat vehicle. The model is an 8-wheel drive, 8-wheel steering system with DC motors to power the vehicle, as depicted in Figure 1.2. The chassis, made put of aluminum, housed a double wishbone suspension system, a driving system, and a steering system with all the essential electronic hardware. Each wheel has its own DC motor to power it and gearbox to reduce the speed and increase output torque. The steering system worked using linear servo system and individual actuators for each wheel of the vehicle. This set-up enabled the vehicle to have multiple steering configurations. The three explored in this paper were the Front Wheel steer, the 4th axe steer, and the All-Wheel steer. The vehicle ran on a CPU interfaced with various controllers and sensors. The electronic components specifications are presented tabularly in the paper. Furthermore, the thesis discusses the development of mapping and path planning algorithms, localization algorithms to equip the vehicle with autonomous navigation.

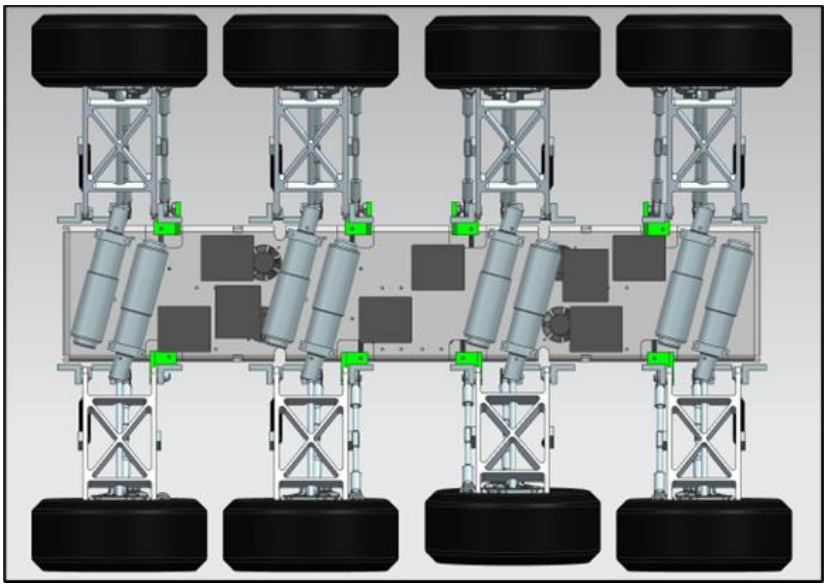

Figure 1-2. Electric powertrain implemented in the Scaled Electric Combat Vehicle [6]

Two distinct control systems, an Active Rear-axle Steering (ARS) and a Torque Vectoring Controller (TVC), were introduced by Ahmed et al. [7] in 2020. TVC is concerned with regulating the scaled vehicle's yaw rate, and the ARS developed by Russell [5] was employed to reduce the side slip angle of the vehicle. The TVC was applied using the Single-Input-Single-Output (SISO) control approach, and Ahmed et al. [8] installed an Optimal Linear Quadratic Regulator (LQR) to regulate the ARS. In a conventional steering scenario, two controllers were used (first two-axle steerable). Using TruckSim software, simulation results were obtained in order to assess two control systems under a range of driving situations, such as varied vehicle speeds and friction surface levels in the Double Lane Change test by Omar et. Al. [9]. According to the simulation results, both controllers improve the stability and dynamic performance of the SECV under different driving circumstances. TVC, on the other hand, exhibits superior stability and maneuverability during the high-speed test than ARS on the dry road surface. On the other hand, ARS is for improved car performance when traveling at a high speed on a slick surface [7].

In 2021, Ahmed et al.[10] investigated four different steering modes to maneuver the vehicle at different speeds. The methods – Conventional front steering, Crab steering, Fixed 3rd axle and All Wheel counter steering – were evaluated using the standard TOP-2-2609 and modified NATO AVTP-1 03-30 maneuvers. The results of the tests are highlighted in the literature. As a result of the aforementioned Active Rear Steering (ARS) stability controller, the constraints on the lateral position tracking, head angle tracking, and control inputs were tightened, resulting in enhanced path following performance. Additionally, the controller highlighted how the rear steering angles played a significant role in achieving zero side slip condition.

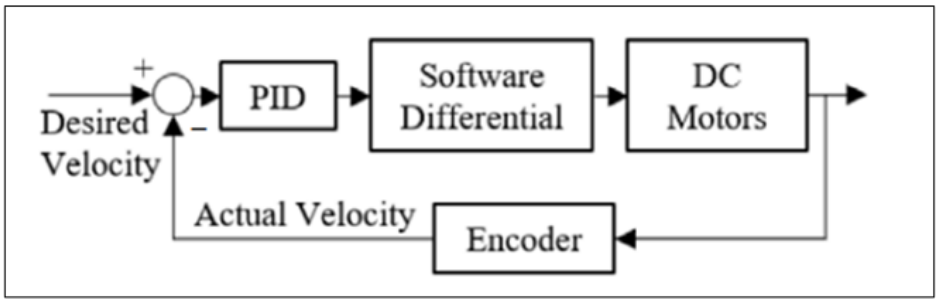

Figure 1-3. Block diagram of PID controller [11]

In 2022, Tan et al. [11] demonstrated that low-level vehicle dynamic control algorithms and high-level path planning are used for autonomous navigation and parking strategies in terms of the 8x8 SECV. Most importantly, a PID controller—which is shown in Figure 1.3—was installed to maintain wheel velocity between the measured value and the desired value. The controller estimates the velocity of Center of gravity (CG) distributed for eight-wheel drive by receiving feedback from the encoder. The primary goals of using a PID controller are to improve steering control and reduce tire slippage [11].

In 2023, Kim et. al. [12] examines the wheel speed management and steering of an entirely custom-built 8x8 scaled electric combat vehicle (SECV) that is designed to meet the low-speed Ackermann condition. Using a portable tachometer, the findings from the wheel angular velocity experiment were confirmed. Linear actuator sensors were used to verify each wheel's steering angle data. The physical findings of the SECV were found to be within a reasonable range of the theoretical data. Wheel speed, center velocity, yaw rate, and eight-wheel steering angles are among the performance measures that were examined during the testing of the conventional two-axle steering setup. This work's unique physical investigation with the continuous Ackermann relationship for eight wheels, which was incorporated into the SECV physical model, is one of its main contributions [12].

Chapter 2. Modelling of the Scaled Electric Combat Vehicle

MATLAB serves as the programming platform for both storing parameters and mathematically modelling the linearized kinematics of the combat vehicle. Additionally, it contains proprietary algorithms essential for generating the controllers employed in this project. On the other hand, Simulink provides a user-friendly graphical interface for modelling and utilizes mathematical solver systems to construct the control structure. Within Simulink, an S-Function is employed to facilitate the import and export of vehicle control data. This data exchange is crucial for conducting software-in-the-loop (SIL) simulations in collaboration with TruckSim. Specifically, Simulink houses the implementation of external electric powertrain models and control systems. These systems rely on the input of vehicle data obtained from the TruckSim S-function. Subsequently, they calculate and apply the necessary control actions to the full vehicle model, creating a comprehensive and integrated simulation environment.

A scaled down electric vehicle model is employed for dynamic simulations, featuring 23 degrees of freedom (DOF) to describe its motion characteristics. These simulations are executed using specialized software called TruckSim© by Mechanical Simulation™, which utilizes 177 ordinary differential equations to compute the vehicle's kinematics and dynamics. This model is a 1:6 model of the original vehicle. The primary body of the vehicle is considered as a rigid structure with six DOF, encompassing three translations and three rotations. The steering system is represented with one DOF, typical for a single-axis steering setup. Additionally, each of the eight wheels on the vehicle is attributed two DOF, one for vertical movement (suspension) and one for spin (rotation). It's important to note that this model is designed to mimic an actual combat vehicle, as depicted in *Figure 1-1*.

2.1 Physical Parameters of Scaled Electric Combat Vehicle (SECV)

A series of tests was conducted, and the physical characteristics of the scaled vehicle were recorded in a MATLAB file. A digital weighing scale was used to measure the weights highlighted in the table below. Manual measurements were also made for the different distances and lengths. On a 2D graph, the front view of the vehicle suspension system was used to calculate the roll center. In order to determine suspension stiffness and damping coefficients, several physical tests were conducted. In order to determine the maximum power, a dynamometer was used. Simulink used the MATLAB file as a reference database for all the parameters when TruckSim simulation was running the SECV. The parameters measured from the original physical model of the vehicle is presented in the *Table 1*.

Parameter	Units	Value
Total weight (including axles and wheels)	Kg	36.9
Sprung mass	Kg	29.94
sprung mass roll inertia (I_{xx})	Kg-m^2	33.798
sprung mass pitch inertia (I_{yy})	Kg-m^2	123.074
sprung mass yaw inertia (I_{zz})	Kg-m^2	136.454
Longitudinal mass center of sprung mass from first axle (X)	mm	307
Lateral mass center of sprung mass (Y)	mm	0
Vertical mass center of sprung mass from ground (Z)	mm	197.5
height (H)	mm	238.3
width (W)	mm	590
Sum of left and right wheels and axle weight for First axle	Kg	1.74
Sum of left and right wheels and axle weight for Second axle	Kg	1.74
Sum of left and right wheels and axle weight for Third axle	Kg	1.74
Sum of left and right wheels and axle weight for Fourth axle	Kg	1.74
Axle 1 (Steering axle reference Position)	mm	0
Axle 2 (x distance from front axle)	mm	199
Axle 3 (x distance from front axle)	mm	410
Axle 4 (x distance from front axle)	mm	614
Maximum Power (max power of each motor is 90W)	kW	0.72
Wheel track width of first axle	mm	525
Wheel track width of second axle	mm	525
Wheel track width of third axle	mm	525
Wheel track width of fourth axle	mm	525
Wheel center height for first axle	mm	91
Wheel center height for Second axle	mm	91
Wheel center height for Third axle	mm	91
Wheel center height for Fourth axle	mm	91
Roll center height for first axle	mm	170
Roll center height for second axle	mm	170

Parameter	Units	Value
Roll center height for third axle	mm	170
Roll center height for fourth axle	mm	170
Tire equivalent spring stiffness (Vertical Force Spring rate)	N/mm	21.29
Full size tire equivalent spring stiffness (Vertical Force Spring rate)	N/mm	550
Suspension spring stiffness of first axle	N/mm	3.34
Suspension spring stiffness of second axle	N/mm	3.34
Suspension spring stiffness of third axle	N/mm	3.34
Suspension spring stiffness of fourth axle	N/mm	3.34
Suspension shock absorber damping coefficient of first axle	kN-s/m	0.1
Suspension shock absorber damping coefficient of second drive axle	kN-s/m	0.1
Suspension shock absorber damping coefficient of third drive axle	kN-s/m	0.1
Suspension shock absorber damping coefficient of fourth drive axle	kN-s/m	0.1
Steering gear box ratio	-	20.4

Table 1. Measured Parameters of SECV

The vehicle is equipped with two steering axles on the front, as shown in *Figure 2-1*. Perpendicular lines at the geometric centers of the four steering wheels and the rear two axles can be plotted to determine the individual steering angle according to the Ackerman condition.

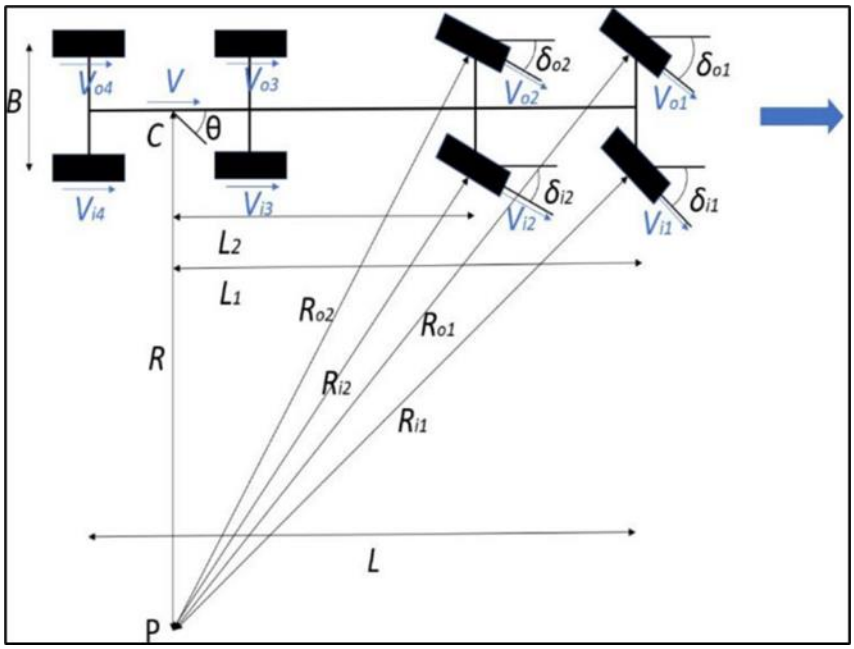

Figure 2-1. Ackermann Steering for 1st and 2nd axle steering

Figure 2-2 depicts the tire's longitudinal force behaviour on the vehicle, while *Figure 2-3* illustrates its lateral force characteristics. Each set of curves in both figures represents how the tire responds under varying normal loads (F_Z). The tire characteristics that were supplied have been incorporated into TruckSim Simulation software in the form of a lookup table. By examining *Figure 2-2*, the specific longitudinal slip value at which the maximum tractive force (F_X) is achieved can be determined. The tire aligning moment is also depicted in *Figure 2-4* with the peak being 61.22 N-m.

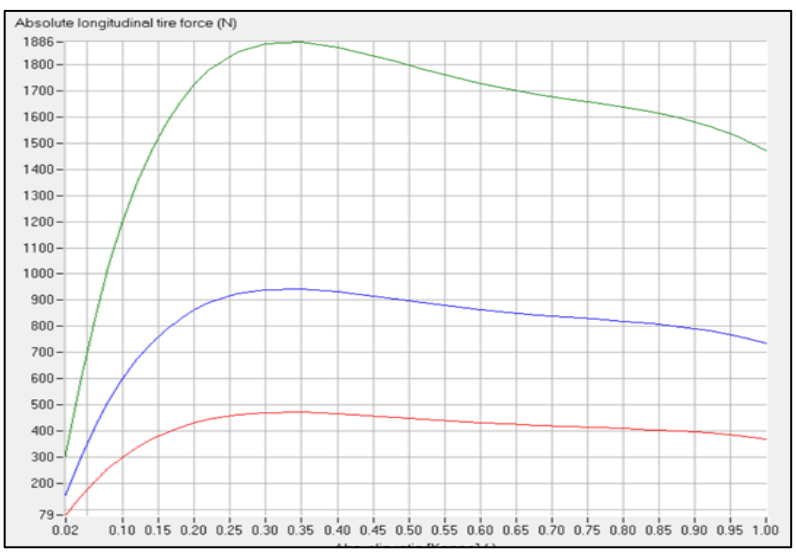

Figure 2-2. Absolute longitudinal tire force of each tire

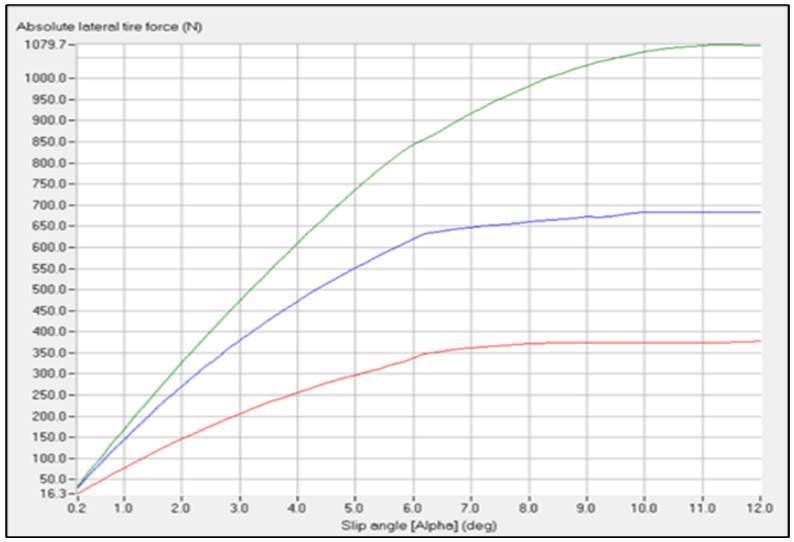

Figure 2-3. Absolute Lateral Force for each tire

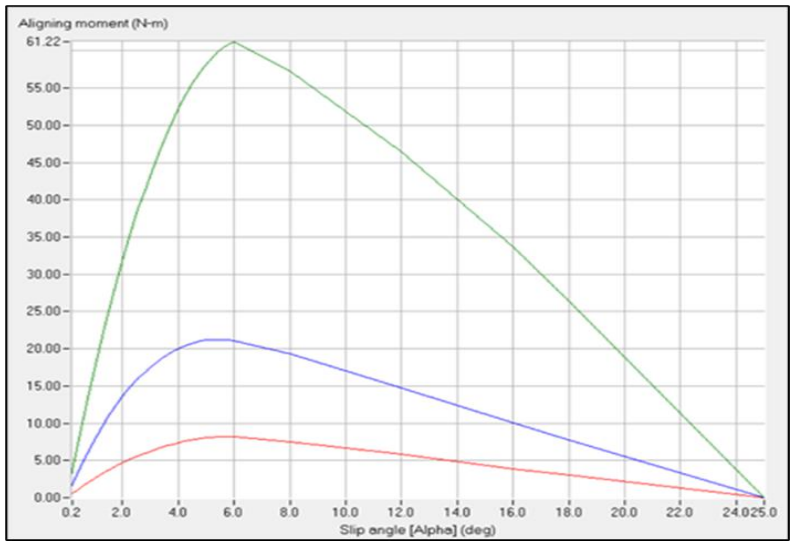

Figure 2-4. Aligning Moment induced in each tire.

2.2 Motor Specifications inputted into MATLAB.

The motor used to propel these vehicles is the Maxron RE motor (Model#285785). There are eight permanent magnet AC motors mounted on the scaled electric combat vehicle's powertrain. The specification of these motors is highlighted in *Table 2*.

No Load Speed	7200 RPM
No load current	188 mA
Nominal Voltage	15 V
Nominal Current	4 A
Max Efficiency	85%
Nominal Torque	74.2 mNm

Table 2. Specifications of each motor used.

2.2.1 MATLAB inputs.

The electric powertrain model is constructed within Simulink and employs a three-dimensional characteristic lookup table that represents the proposed motors. This lookup table is used to calculate the output motor torque. *Figure 2-5* illustrates the electric motor lookup table utilized in this project, which relies on two main inputs: motor rotational speed and motor current. Each curve within the table corresponds to a specific magnitude of the motor current input.

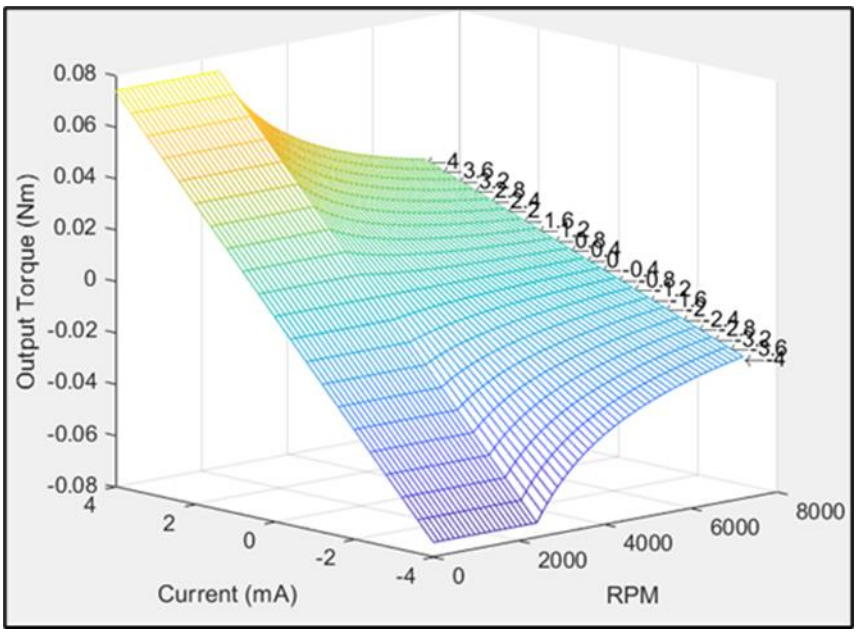

Figure 2-5. Output Torque vs Current vs RPM of each motor.

To calculate the output motor torque, Simulink utilizes the provided wheel speed and motor current as inputs. It then performs interpolation within the lookup table, taking into account the specified values of wheel speed and motor current, and generates the corresponding output motor torque. Notably, the lookup table also includes negative current curves, which account for reverse spinning. This is particularly important since the rotational speed is represented as a scalar value within the TruckSim environment, and the negative current curves enable the model to handle reverse motion appropriately. When MATLAB runs the simulation, it reads the look-up table from a text file.

2.3 *Powertrain Design Implemented in Simulink*

The following sections discusses the development of the all-electric powertrain in MATLAB/ Simulink. The powertrain consists of two main parts – the motor current block and the motor block itself.

2.3.1 General Architecture

TruckSim supplies essential driver and vehicle operation information continuously during a test procedure. This data serves as input for each of the controllers implemented using Simulink. The controllers process this information, and the resulting processed data is subsequently transmitted back to TruckSim in the form of vehicle actions, such as wheel torque and wheel steering angles. The basic control structure employed by Simulink is depicted in *Figure 2-6*.

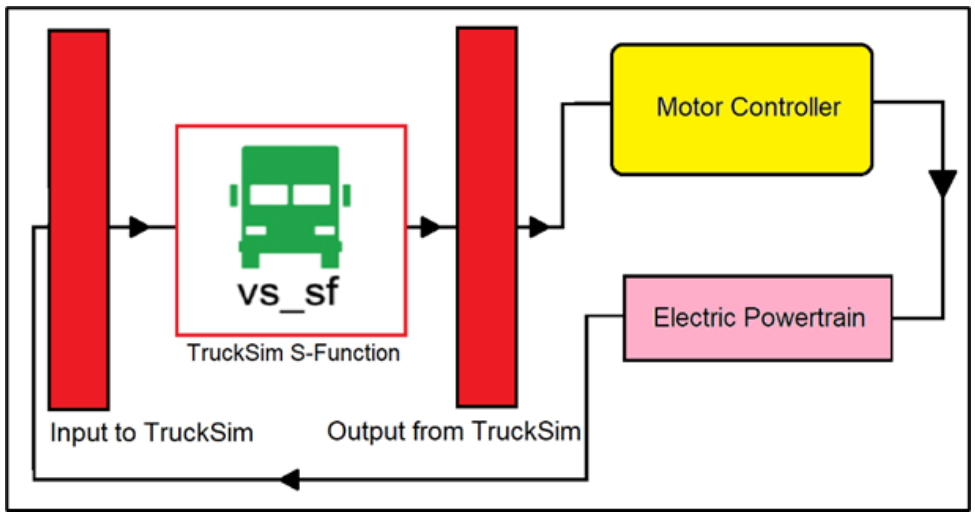

Figure 2-6. General Architecture of Simulink file developed.

2.3.2 Vehicle Velocity Controller Block Design

Figure 2-7 illustrates the internal structure of the forward speed controller used for regulating a vehicle's speed in a simulation environment like TruckSim. It employs a PD controller and an open-loop throttle controller, with a conditional switch determining which one is active based on the simulation's requirements.

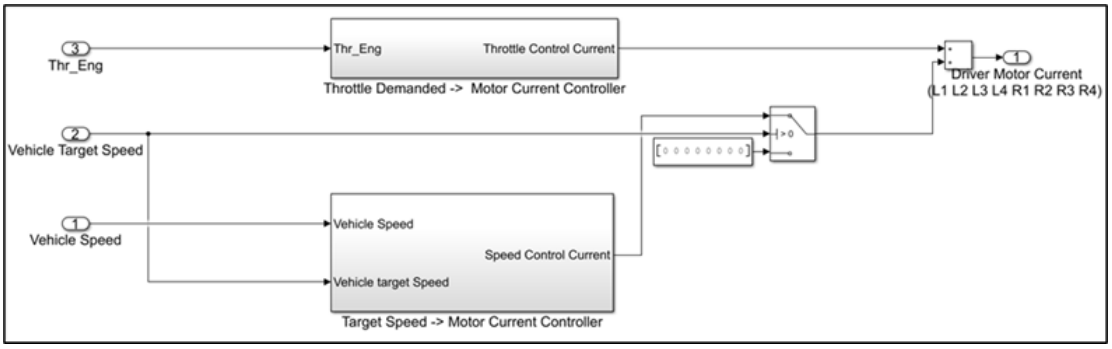

Figure 2-7. Simulink Architecture for motor current derivation

If a constant target speed isn't set within the TruckSim environment, the switch alters its function to turn off the PD controller and turn on the open-loop throttle control. In this situation, the system reads the throttle input from the internal TruckSim driver model, which ranges from 0% (indicating no throttle) to 100% (indicating full throttle). The system then calculates the throttle input as a percentage of the maximum allowable input motor current and sends this value equally to all eight wheels through the wheel torque distribution system.

When a constant target speed is designated, the TruckSim environment sends a zero-throttle signal to the open-loop controller, effectively rendering it inactive. Meanwhile, the target speed and the actual vehicle speed are obtained as input signals from the TruckSim environment. These signals are used to calculate an error signal for the PD controller, which has been fine-tuned in TruckSim to produce an appropriate control action in the form of motor current within the specified input limits. Regardless of the mode of operation, the speed controller evenly distributes the mean forward driving current to each wheel in the torque distribution system, ensuring balanced power distribution to all wheels.

2.3.3 Motor Block Design

To calculate the required motor rotational speed for a lookup table based on a single electric motor, the rotational inertias of the wheel and the motor hub must be considered. Based on this, if we isolate the effect of the wheels on the ground, the net motor torque would be:

$$T_{net} = T_m - I_m \alpha_m$$

Where T_{net} is the net Torque, Tm is the torque from the motor, I_m is the rotational inertia of the motor, and αm is the angular acceleration of the motor. By taking into account the tractive force (F_x) and the motor reduction, the wheel's net torque becomes

$$T_{net} n_m - F_x r_{ef} = I_w \alpha_w$$

Where I_w is the rotational inertia of the wheel, αw is the angular acceleration of the wheel, ref is the effective rolling radius of the tire and nm is the motor gear reduction ratio. Isolating for αw and integrating the remaining equation gives us the rotational speed of the wheel.

$$\omega_w = \int \alpha_w = \int \left[\frac{T_{net} n_m - F_x r_{ef}}{I_w}\right] dt$$

When the motor gear reduction ratio is multiplied by the wheel rotation speed, the required motor rotational speed can be obtained.

$$\omega_m = \omega_w n_m$$

In *Figure 2-8*, you can observe the equations that were previously described, and they have been implemented in Simulink. The process involves reading the tractive force (F_X) from the TruckSim environment to perform a continuous calculation of the motor's rotational speed.

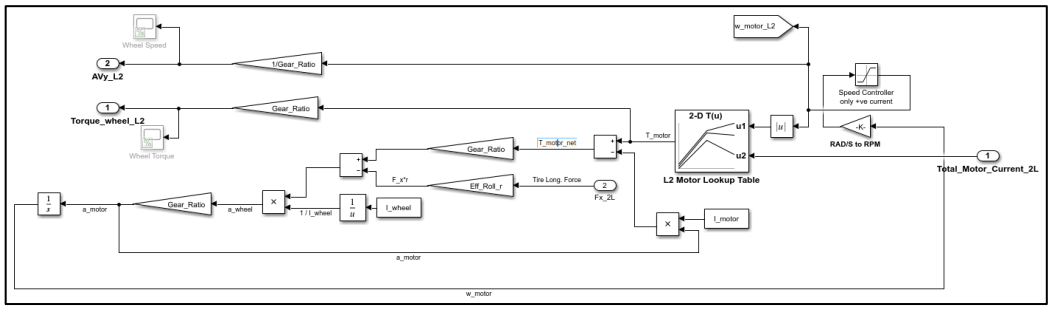

Figure 2-8. Simulink Architecture for individual motor

To send data back to the TruckSim environment, two key calculations are carried out:

Motor Torque Adjustment: The motor torque is multiplied by the reduction factor to obtain the wheel torque. This step ensures that the torque applied to the wheels accounts for the reduction in the powertrain system.

Motor Speed Adjustment: The motor speed is divided by the reduction factor. This adjustment is made to align the motor's rotational speed with the actual wheel speed, considering the effects of the reduction mechanism.

These adjustments are essential for maintaining consistency and accuracy in the simulation, allowing data to be exchanged between Simulink and the TruckSim environment effectively. *Figure 2-9* illustrates the powertrain model developed in Simulink. The model does not have an Absolute Braking System (ABS) or a Traction Control System (TCS).

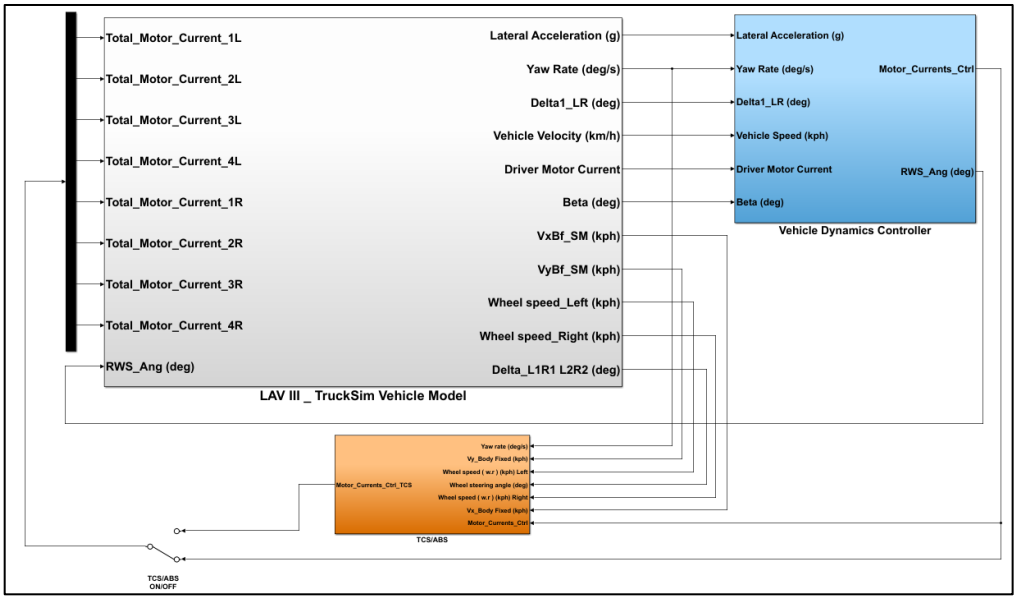

Figure 2-9. Simulink Architecture for electric powertrain

Chapter 3. Validation of the Scaled Electric Combat Vehicle

The test chosen to validate the virtual model of the SECV is the Double Lane Change (DLC) test. The Double Lane Change (DLC) test is one of the best methods in vehicle dynamics analysis because it simulates an emergency maneuver that replicates real world driving scenarios [13]. The test is preferred because it provides objective and repeatable results through more structured tests. Additionally, open-loop tests are preferred because they are not affected by the driver's influence. The double lane change test is a closed-loop test, but it is still preferred because it is standardized and can be conducted with and without electronic stability programs. The test is conducted according to standard ISO 3888-2, which defines the double-lane change maneuver to test the vehicle's ability to avoid obstacles. The driver accelerates until the vehicle reaches a certain speed, then quickly changes lanes twice in opposite directions while maintaining control of the vehicle.

3.1 Vehicle Model and Test Apparatus Specifications

In order to carry out the test, the following hardware was used. A laptop, equipped with an Intel Core-i5 processor and 16 GB of RAM, was mounted on top of the scaled electric combat vehicle. It serves the purpose of data recording, control, and potential real-time data analysis. The vehicle was equipped with an Inertial Measurement Unit (IMU), specifically the RSX UM7 Orientation Sensor, which had three sub-sensors: an Accelerometer, Magnetometer, and Gyroscope. This IMU provided essential data, including yaw rate, to assist in controlling the vehicle's orientation. For navigation and position tracking, the vehicle was equipped with a GPS unit, the Locosys MC-1513, which delivers position and velocity data. It offers a positional accuracy of 3 meters and can measure velocities of up to 515 meters per second. Human control of the vehicle was facilitated by a Logitech F710 USB controller, allowing the driver to generate commands for steering and velocity adjustments. These commands are then transmitted to the main Arduino unit. The vehicle's control system relied on three Arduino Mega 2560 microcontrollers. One functioned as the main controller, receiving input commands from the remote controller. The other two sub-Arduinos were dedicated to precise control of the eight-wheel steering using closed-loop PID control algorithms. Linear actuators were employed to control the steering rods, and they incorporated potentiometers for feedback, enabling accurate closed-loop position control. These actuators were each powered by 12V NIMH batteries. To manage the vehicle's velocity, four Roboteq SDC2130 motor controllers were installed. One of these served as the master controller, receiving velocity commands from the main Arduino, and subsequently distributing them to three sub-motor controllers. These controllers use PID control for closed-loop speed regulation of the eight wheels. To provide feedback for the PID controllers within the motor controllers, eight encoders (AMT10 Rotary Encoders) were mounted on the drive shafts, measuring the real-time speed of the eight wheels. Power for various vehicle components was supplied by LiPo batteries (Gens ace 6200mAh 14.8V 45C), ensuring efficient operation of the motor controllers, linear actuators, and other subsystems. This setup was designed

for the development and testing of the scaled electric combat vehicle, with a primary emphasis on precise steering and velocity control. The combination of IMU, GPS, remote control, and multiple controllers enabled accurate monitoring and control of the vehicle's movements.

3.2 Test Setup Specifications

The path and cone layouts utilized for the DLC test in this work are depicted in *Figure 3-1*. The testing standard specifies that cone spacing & path parameters depend on the vehicle's physical specifications. For the vehicle used in this study, the DLC test has been specifically modified. The SECV must not come into contact with any one of the cones throughout the test, regardless of size. For the current test, the length of the path was 20.16m with a displacement of 1.8m from the initial path of the vehicle. A rectangular perimeter was set up with the four aforementioned sensors (to track the GPS, Locosys MC-1513) placed at each corner of the perimeter. The corner sensors were first calibrated to track the precise position of the GPS sensor. The perimeter, along with the path of the vehicle were physically measured using a tape. The vehicle was set to a maximum speed of 1km/h for the first iteration and the test was carried out. The results were recorded, and the test was repeated for the iteration with the maximum speed set to 2 km/h.

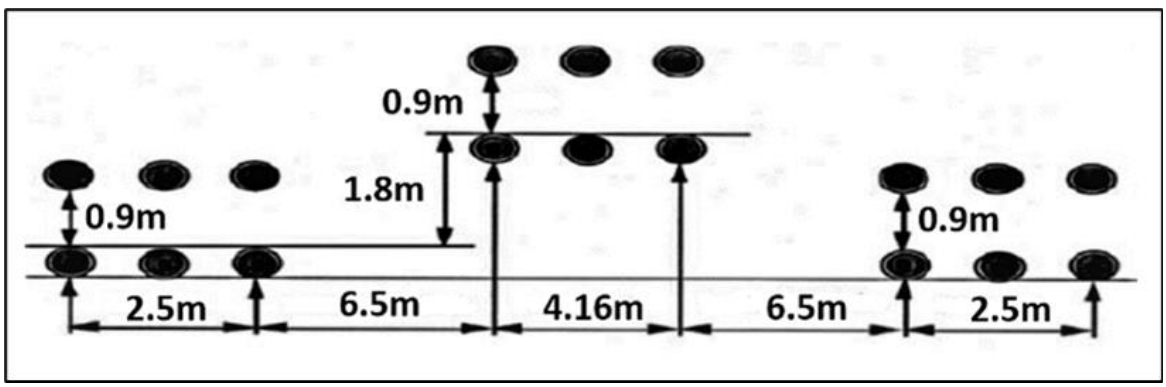

Figure 3-1. Schematic of path setup for the Double Lane Change (DLC) test

On TruckSim Mechanical Simulator, the exact conditions used for the experimental road test was setup. Being a complex software, more data was extracted from the software. In order to carry out a validation of the virtual model, parameters such as the individual wheel angles, the longitudinal velocity and the yaw rate were compared for both the simulation and the experimental tests. The road surface chosen had the coefficient of friction as 0.8, the same as the test run on the simulator. Because this is a 1:6 scaled replica of the original vehicle, the speeds of 1km/h and 2km/h roughly translate to 6 km/h and 12km/h for the original combat vehicle, data of which was available. The DLC path chosen for the original vehicle was also scaled down accordingly and applied to the scaled electric combat vehicle (SECV). *Figure 3-2*. compares the path in the simulation environment to the experimental path used.

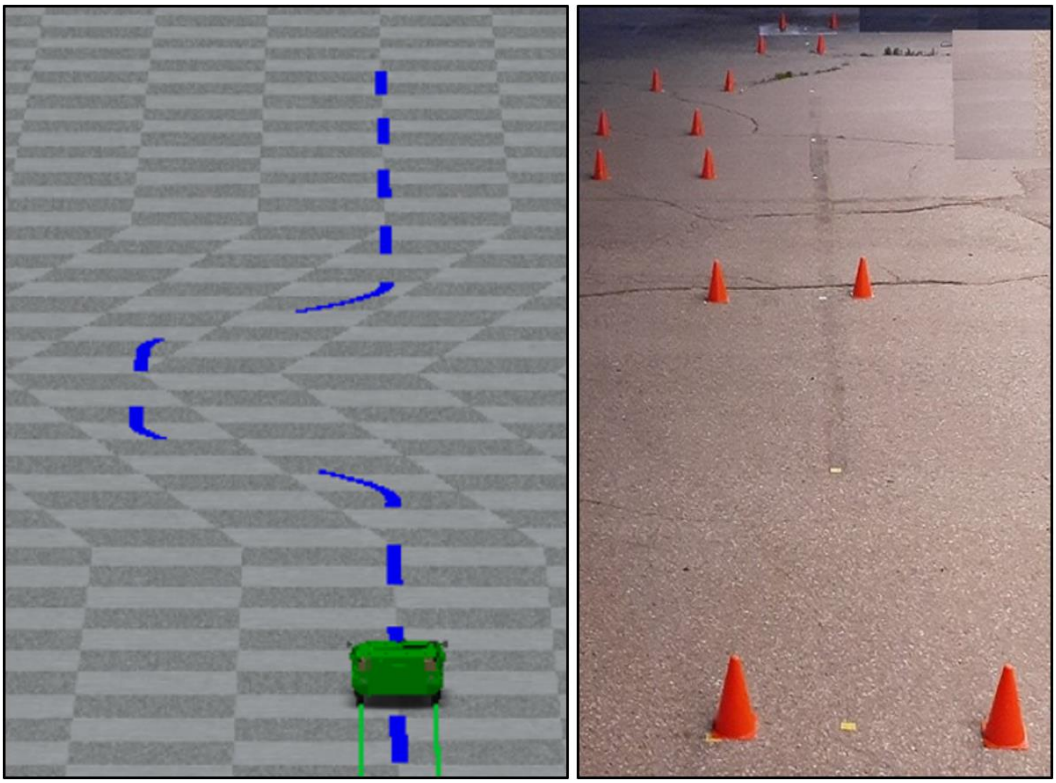

Figure 3-2. (a) Simulation and (b) Experimental path followed by the SECV

Chapter 4. Results and Discussions

After the simulation test was completed, an Excel file with the simulation results was exported. After the data was organized, the necessary information was taken out. Then, Microsoft Excel line graphs were used to illustrate the simulation results. After the experimental tests were executed, the experimental results were extracted from the sensors and were treated for any noise interferences. The data was then exported and visually depicted using Excel too. A comprehensive comparison between the simulated data and the experimental data is presented below.

4.1 Double Lane Change Test at 1km/h.

Figure 4-1 illustrates the comparison between the longitudinal velocities of both the simulation and the experimental results, with the red line representing the simulation speed and the blue line depicting the experimental speed. From the data, it is clear that the fluctuation in the simulation results is minimal because the simulator tries to maintain a constant speed. However, the velocity from the experiment data has a lot of fluctuations because of the noise interference in the GPS system. Further research of the paper can employ a better and accurate GPS sensor that doesn't pick on noise interference. This will give the researchers a more refined data to study. The speed in the experiment has an average of 0.89 km/h, which is 0.11 km/h less than the average speed obtained by simulation (1 km/h).

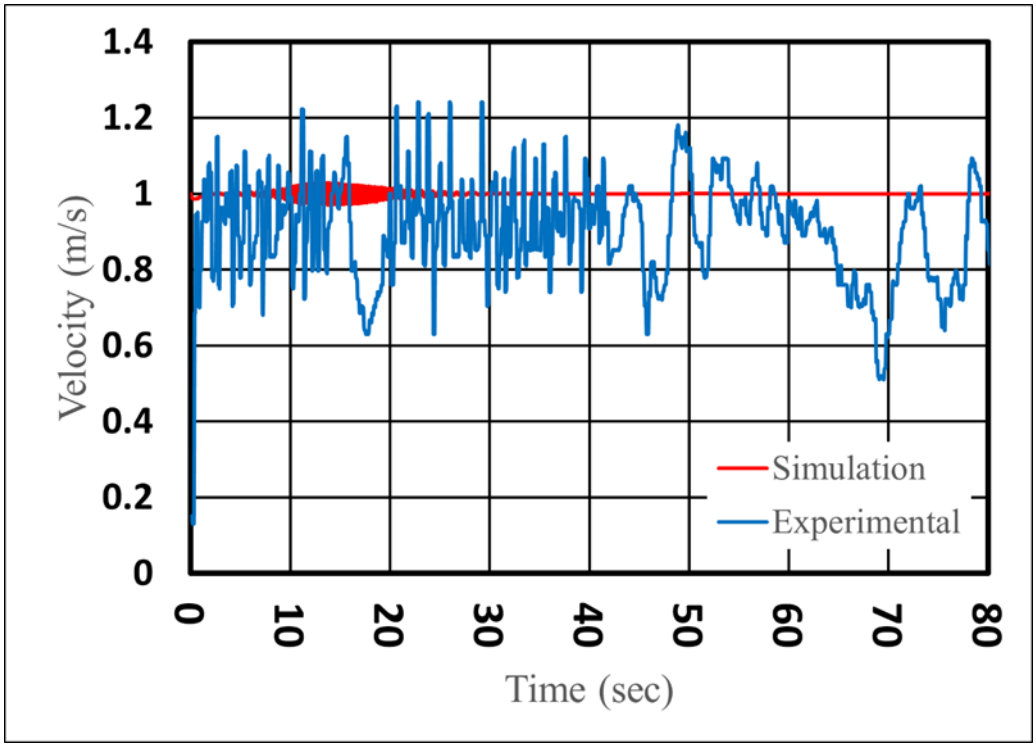

Figure 4-1. Rate of experimental velocity and simulation velocity at 1km/h

Figure 4-2 and *Figure 4-3* depict the eight-wheel angles of the scaled vehicle in the experimental test and the simulation test respectively, during a DLC maneuver on dry asphalt, allowing for a comparison between the simulated and physically obtained data. The graphs in *Figure 4-2* and *Figure 4.3* depict almost identical plots, although there are minor variations in the maximum wheel angles, which are around 0.5 and 1.5 degrees for positive and negative values, respectively. The maximum angle is experienced by the First axle – Left wheel of 7.70 degrees in the experimental results. For the simulation data, the same wheel experiences the maximum angle, but at 4.75 degrees.

A mechanical problem in the top control arm of the SECV is the reason for the discrepancies between the experimental and simulation data for the angles generated in each wheel. This also causes a slight misalignment in the wheels of the SECV. Because of this, it was challenging for the driver to operate the SECV precisely along the desired path. Consequently, these mechanical issues are the reason for the differences in the trajectory of the vehicle and the projected trajectory. Future variations in the eight-wheel angles can be reduced by increasing the precision of these mechanical systems.

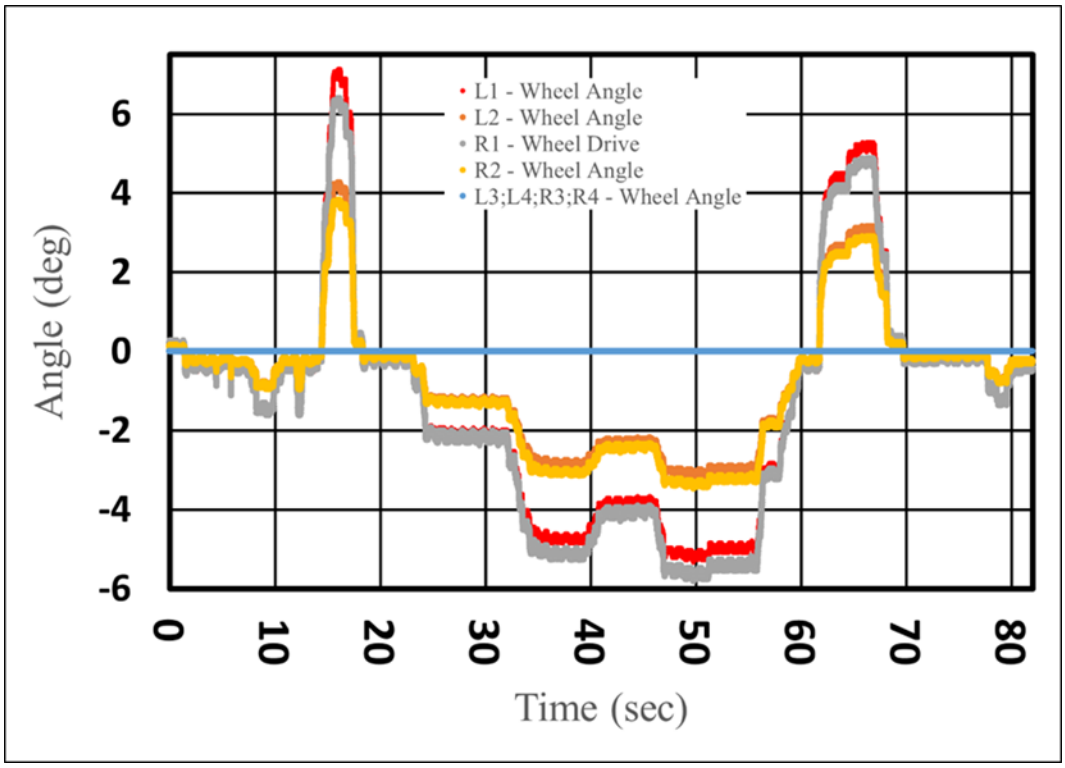

Figure 4-2. Angles induced in each wheel during experiment at 1km/h.

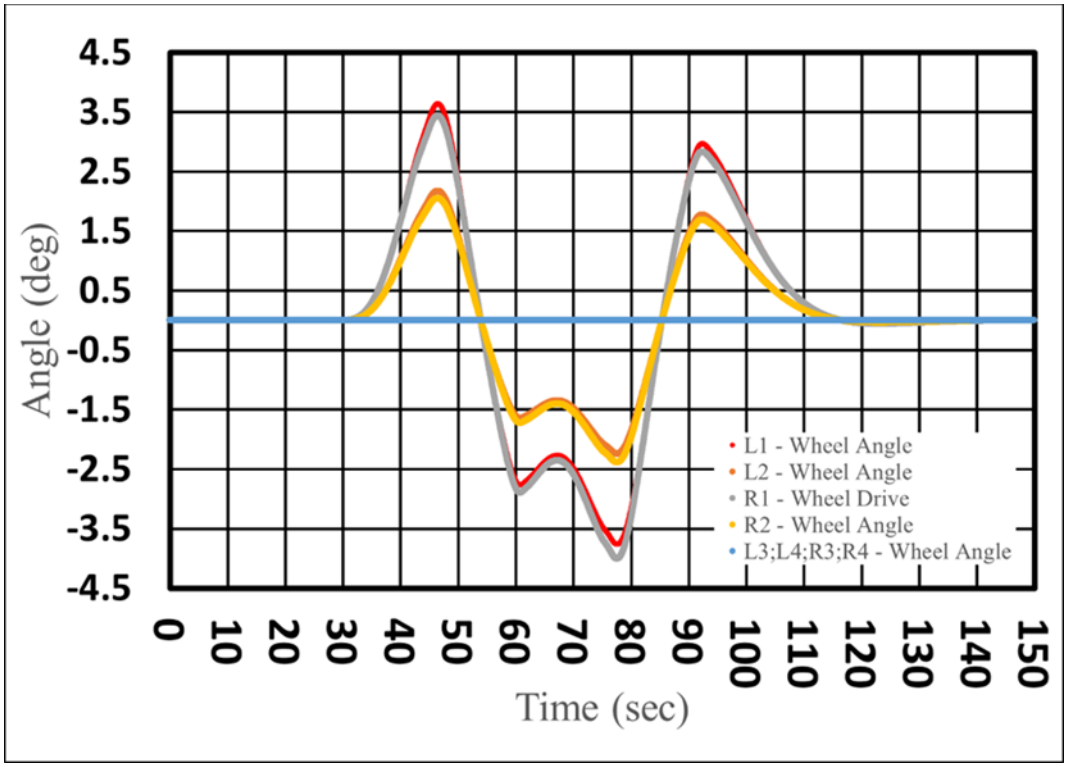

Figure 4-3. Angles induced in each wheel during simulation at 1km/h.

Figure 4-4 illustrates the results of the yaw rate of the experiment that were physically recorded while *Figure 4-5* shows the change of yaw rate with time for the DLC simulation test. The computed yaw rate and the experimentally observed yaw rate are roughly identical, as seen in *Figure 4-6*. There is a difference of 1-2 rad/s in the peaks of the simulated and experimental results. The experimental data displays a peak of 4.1 rad/s while the simulation data peaks at 1.85 rad/s. Furthermore, *Figure 4-6* exhibits a little move to the right in the experiment curve of the yaw rate. The aforementioned mechanical errors that caused the difference in the wheel angles for the simulation and experiment also account for the discrepancies in yaw rates between the two.

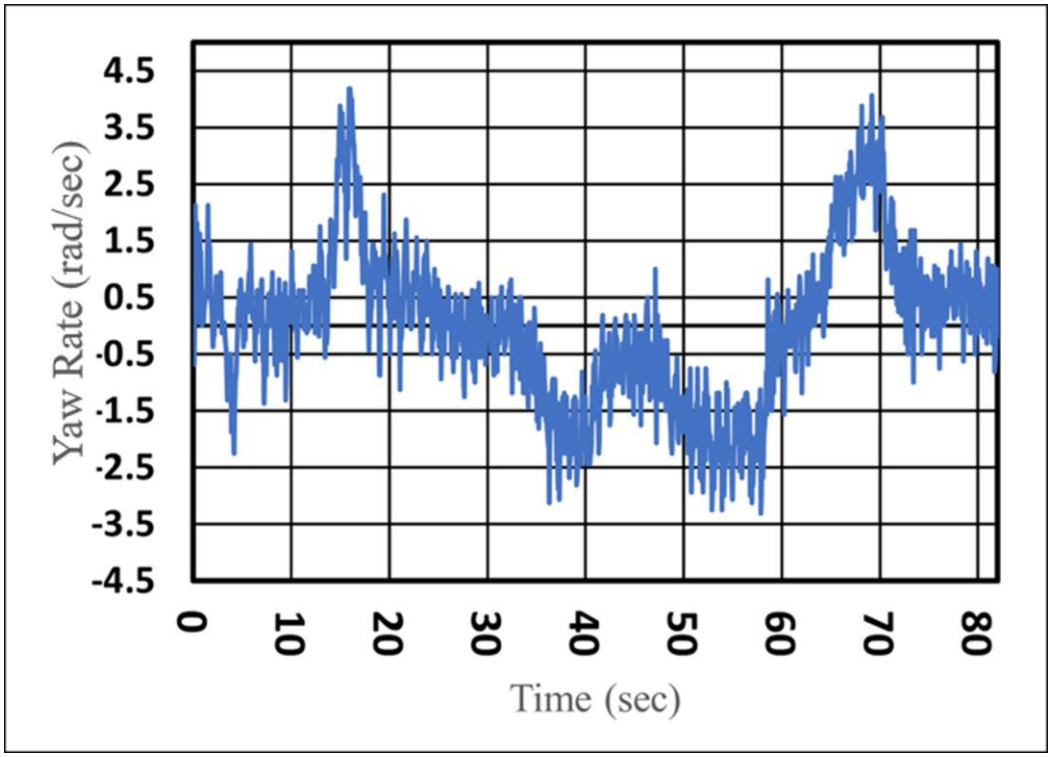

Figure 4-4. Yaw rate experienced in the vehicle during experiment at 1km/h.

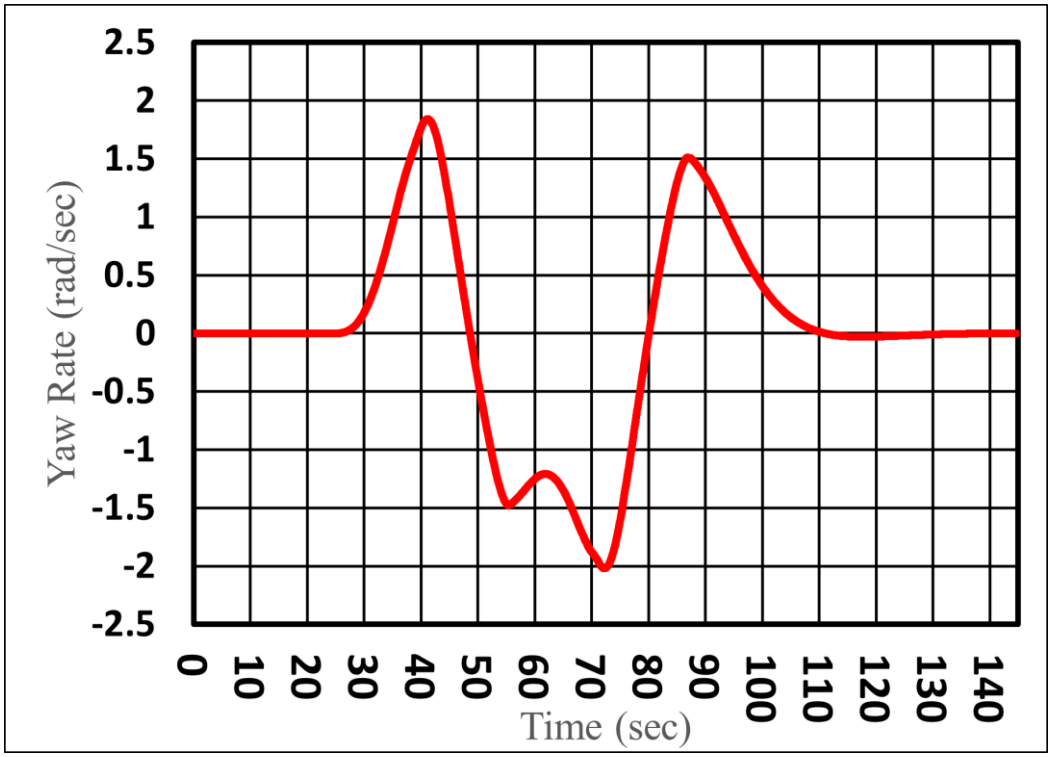

Figure 4-5. Yaw rate experienced in the vehicle during simulation at 1km/h.

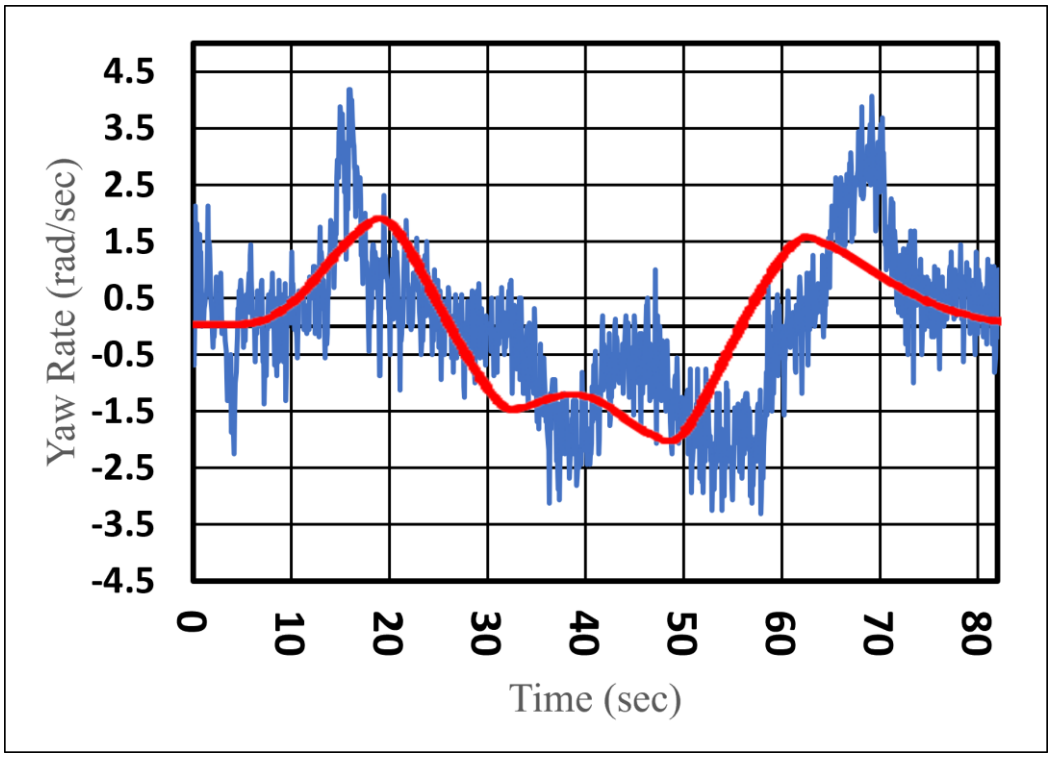

Figure 4-6. Comparison of yaw rates during Experiment vs Simulation at 1km/h

4.2 Double Lane Change Test at 2km/h

In *Figure 4-7*, the red line indicates the simulation speed, while the blue line indicates the experimental speed, illustrating the comparison of the longitudinal velocities between the simulation and experiment data for 2 km/h. Like the test at 1km/h, the experimental data undergoes fluctuations while the simulated data is very close to 2km/h. This is due to the previously mentioned noise interference in the GPS system. Figure 4.6 shows the average longitudinal velocity of the experimental result, which is 1.87 km/h, 0.13 km/h less than the desired speed. At 2 km/h, the speed error percentage is 6.5%, which is lower than the error percentage at 1 km/h (11%). The results show that when the SECV is tested at greater speeds, the GPS sensor becomes more accurate and has less velocity error.

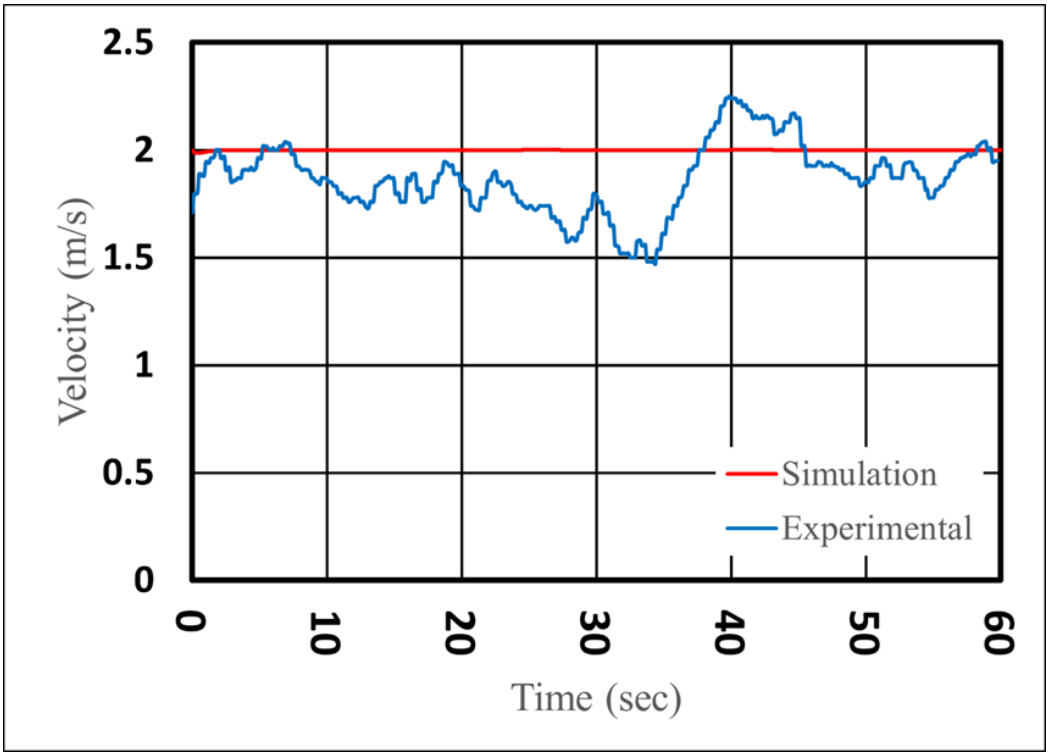

Figure 4-7. Rate of experimental velocity and simulation velocity at 2km/h

Figure 4-8 represents the angles generated in each of the wheels during the experimental test while *Figure 4-9* gives a picture of the angles generated during the simulation test for 2km/h. While the plots in Figure 4.7 and Figure 4.8 are roughly similar, there are some differences in the peaks, with the difference being 2-3 degrees on either side. The discrepancies between the simulated data and experimental data for the wheel angles can be attributed to mechanical errors that were previously discussed in the DLC at 1 km/h speed test. This time, however, the shift to the right does not occur, like it did in the 1km/h DLC test.

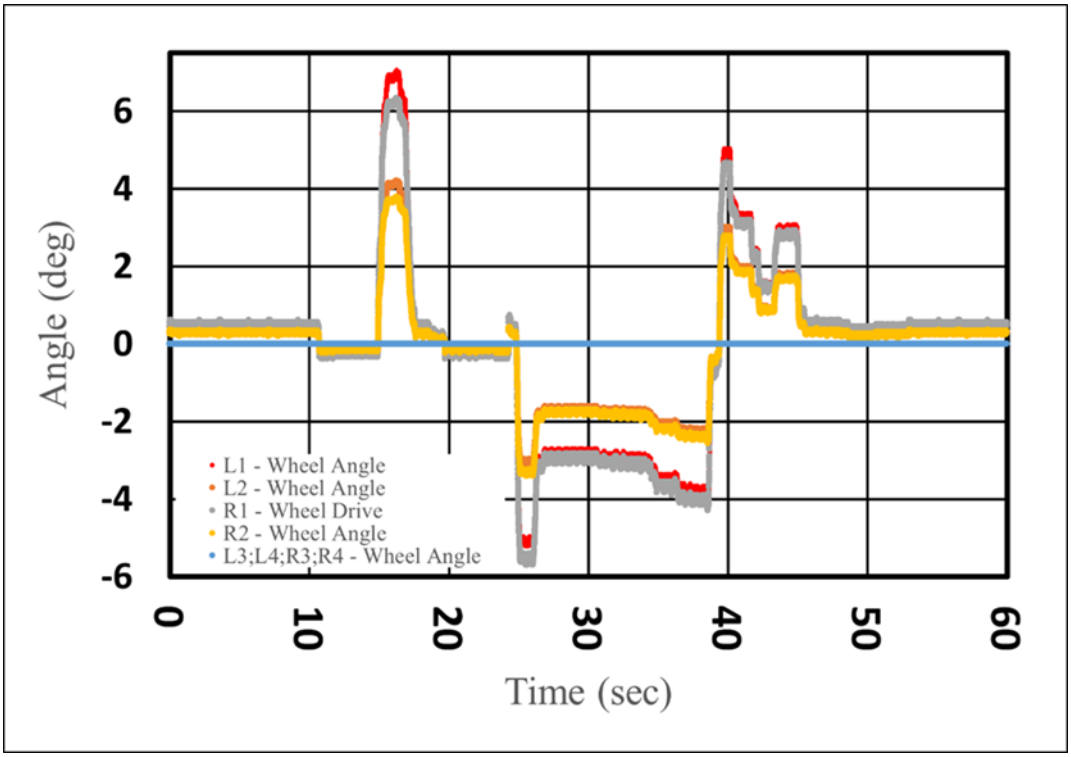

Figure 4-8. Angles induced in each wheel during experiment at 2km/h.

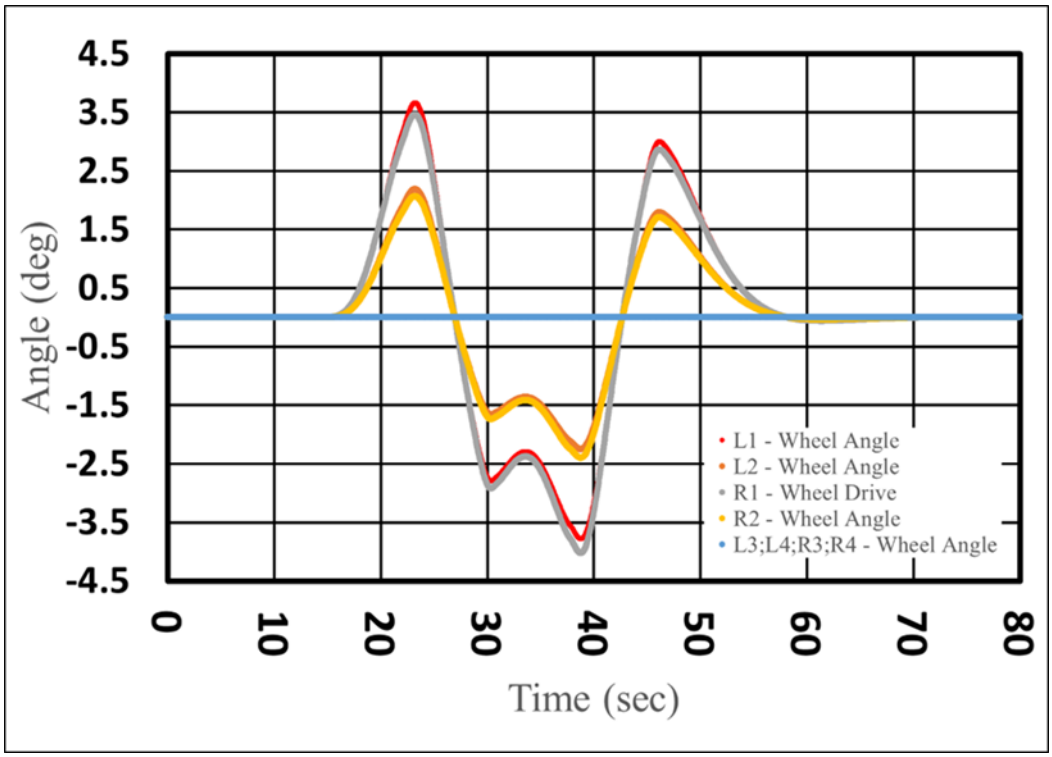

Figure 4-9. Angles induced in each wheel during simulation at 2km/h.

Figure 4-10 shows the yaw rate of the DLC test results obtained from a virtual simulation and *Figure 4-11* shows the results of the physical testing at a speed of 2 km/h. A comparable graph pattern between the simulated and experimental yaw rates is illustrated in *Figure 4-12*. The simulation data peaks at 3.8 deg while the experimental data peaks at 7.5 deg. At 2 km/h, both the graphs still follow a similar trend line, but the discrepancies between the simulation and experiment's highest results are greater than those of 1 km/h. This is because the little mechanical errors become more noticeable at these speeds.

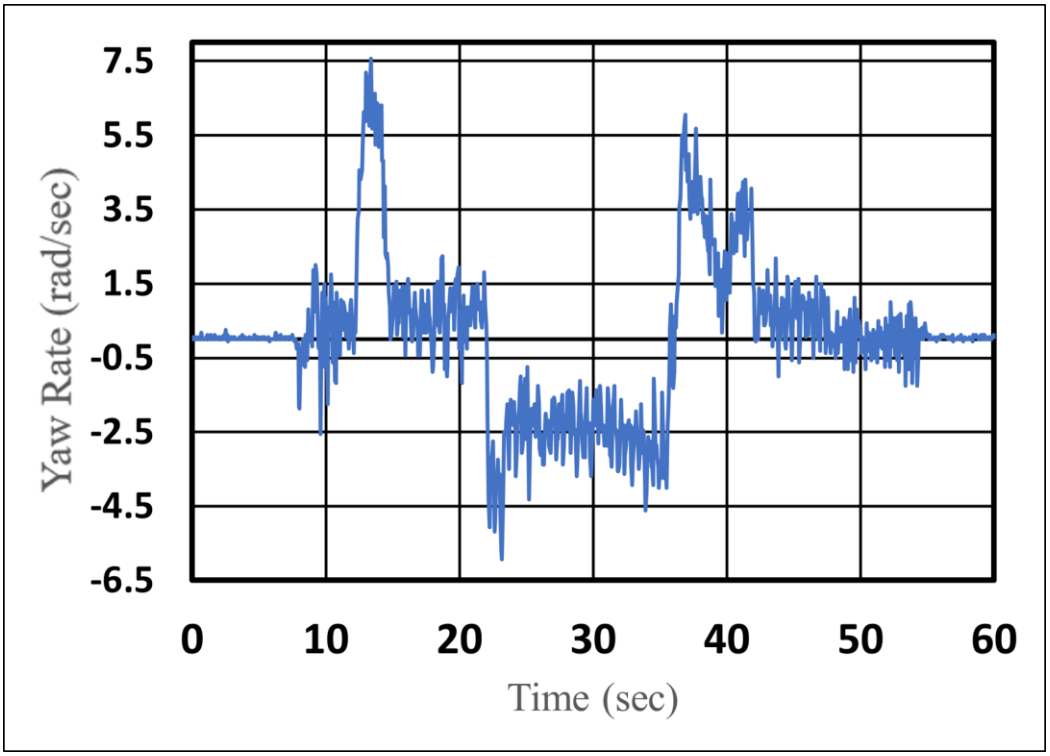

Figure 4-10. Yaw rate experienced in the vehicle during experiment at 2km/h.

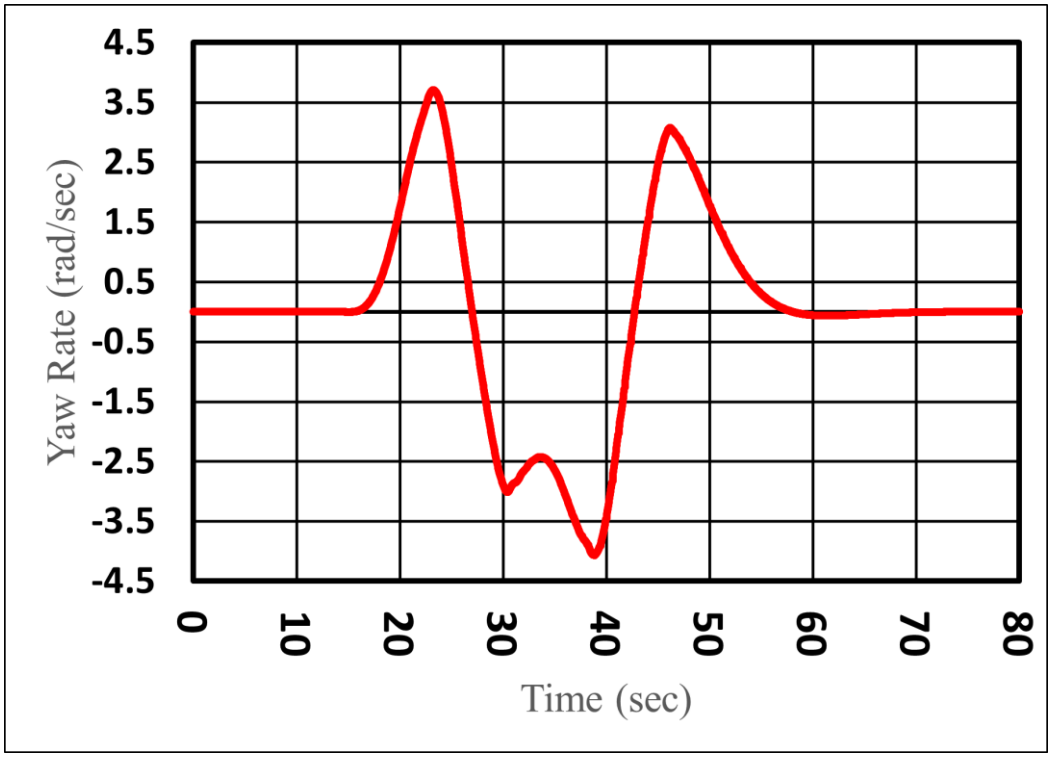

Figure 4-11. Yaw rate experienced in the vehicle during simulation at 2km/h.

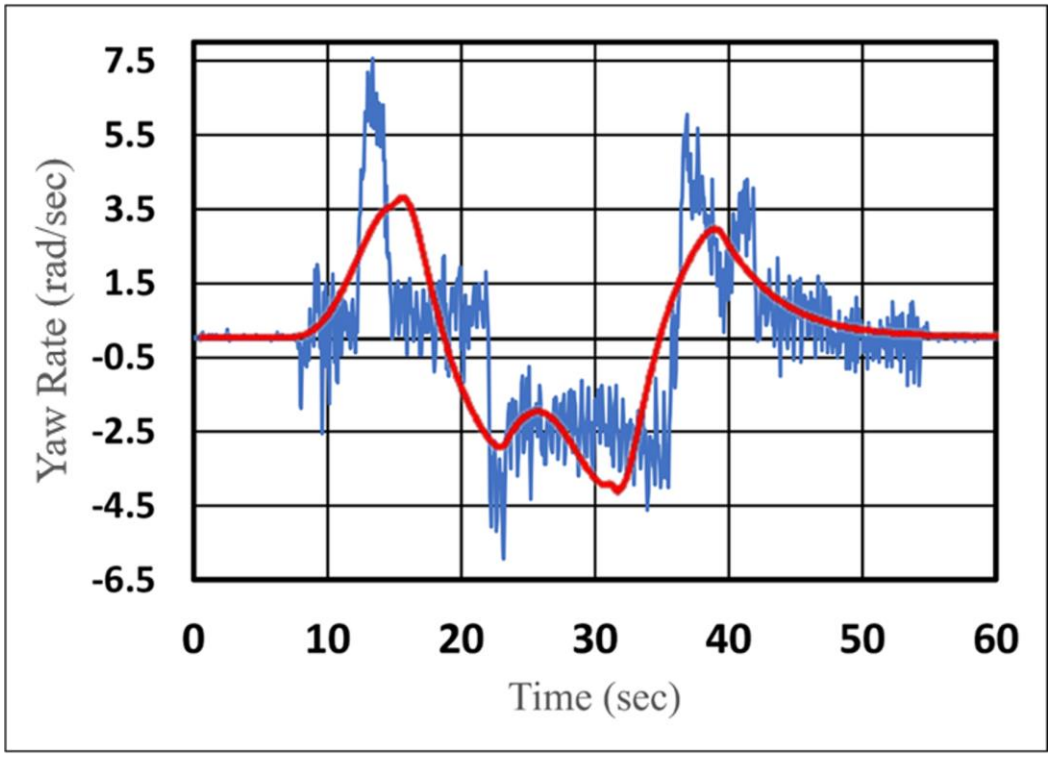

Figure 4-12. Comparison of yaw rates during Experiment vs Simulation at 2km/h

Chapter 5. Conclusions and Future Work

In this study, a virtual model of the Scaled Electric Combat Vehicle (SECV) was created using MATLAB/ Simulink and was subjected to Simulation using TruckSim Modelling and Simulation software. The virtual model created, like the actual SECV, is an 8x8 drive vehicle, with each wheel having its own motor for power, and a linear actuator for steering. The steering system in the vehicle (and the virtual model) is the traditional setting where the first two axles are steerable.

The virtual SECV model was then validated by conducting experiments on the actual SECV. The comparison between the simulation data and the experimental data was done to validate the model. In order to validate the virtual model, the following parameters were considered – the longitudinal velocity of the vehicle; the angles generated in each of its wheels, and the yaw rate generated in the vehicle. The Double Lane Change (DLC) test was chosen to obtain these parameters. The test was conducted using two different longitudinal velocities – 1km/h and 2km/h.

The results of the simulation and experiment were compared. The velocities in both tests were steady for the simulation results, while there were fluctuations in the experimental velocities. This was due to the GPS tracker picking up noise from the environment. Filtering of the data was done to remove the influence of the noise as much as possible. There is a slight difference in the results for the wheel angles due to a mechanical issue in the actual model of the SECV. Overall, the plots look very similar for both velocities with the yaw rate in both tests also had a slight error, with the 2km/h test showing more error. This was due to the fact that at higher speeds, the mechanical issues in the vehicle model were apparent. For the future, better equipment such as the GPS sensor, the IMU, etc. can be updated to get a lot of other parameters. The vehicle is currently driven using a remote control. It can be upgraded to a path following mechanism to eliminate the human intervention in the experiment. For the virtual model, different steering strategies can be implemented to improve the mobility of the vehicle. Different controllers can be developed to control the stability and dynamics of the vehicle. These controllers can first be analyzed on the virtual model before being implemented in the actual SECV. Ultimately, this research will result in a validated virtual model of the scaled down 8x8 electric combat vehicle that will be used for further research and testing of the full size 8x8 combat vehicle.

REFERENCES

1. Hossam, R. (2014). Torque Control Strategy for Off-Road Vehicle Mobility. *Faculty of Engineering and Applied Science University of Ontario Institute of Technology Oshawa, Ontario, Canada*.

2. D'Urso, P. (2016). *Development of H∞ control strategy for a multi-wheeled combat vehicle* (Doctoral dissertation, University of Ontario Institute of Technology).

3. Odrigo, A. (2017). *Development of multi-wheel drivetrain control system for future electric combat vehicle* (Doctoral dissertation).

4. Omar, M., & El-Gindy, M. (2021). *Direct Yaw Control Based on Optimal Longitudinal Tire Forces for 8× 8 Combat Vehicle* (No. 2021-01-0261). SAE Technical Paper. 5. Russell, B. (2018). *Development and analysis of active rear axle steering for 8x8 combat vehicle*. University of Ontario Institute of Technology (Canada).

6. Tan, A. H. (2019). *Design and development of an autonomous scaled electric combat vehicle* (Doctoral dissertation).

7. Ahmed, M., El-Gindy, M., & Lang, H. (2020, July). Handling performance of an 8x8 combat vehicle. In *The International Conference on Applied Mechanics and Mechanical Engineering* (Vol. 19, No. 19th International Conference on Applied Mechanics and Mechanical Engineering., pp. 1-13). Military Technical College.

8. Ahmed, M., El-Gindy, M., & Lang, H. (2022). A Novel Coordination Method for an Integrated Chassis Controller of an 8x8 Combat Vehicle. *SAE International Journal of Advances and Current Practices in Mobility*, *4*(2022-01-0353), 1250-1263.

9. Omar, M. (2021). *Enhancement of lateral stability for a multi-wheeled combat vehicle using various control strategies*. University of Ontario Institute of Technology (Canada).10. Aboelfadl Ahmed, M. (2021). *Integrated chassis control strategies for multi-wheel combat vehicle* (Doctoral dissertation). 11. Tan, A. H., Peiris, M., El-Gindy, M., & Lang, H. (2022). Design and development of a novel autonomous scaled multiwheeled vehicle. *Robotica*, *40*(5), 1475-1500.

12. Kim, J., El-Gindy, M., & El-Sayegh, Z. (2023). *Development of Novel Steering Scenarios for an 8X8 Scaled Electric Combat Vehicle* (No. 2023-01-0106). SAE Technical Paper.

13. Bîndac, I. M., Bradley, S., Roșca, P., Pupăză, C., & Giurgiu, T. (2022). Theoretical and experimental research on the double lane change maneuver. In *MATEC Web of Conferences* (Vol. 373). EDP Sciences.